

Wnt inhibition may limit human salivary gland cancer progression

Anita Joy*, Donald Reed, Aaron Altman, Kathryn Carter, Joshua Welborn

Joy A, Reed D, Altman A, et al. Wnt inhibition may limit human salivary gland cancer progression. *J Can Res Metastasis*. 2018;1(2):18-22.

β -catenin is a multifunctional protein in the Wnt pathway, and acts as an intermediate for the association of the plasma membrane with the actin cytoskeleton, through binding E-cadherin and α -catenin. Its role as a linker protein between cells is crucial in maintaining E-cadherin's adhesive properties. We aimed to evaluate β -catenin's role in indirectly regulating cell-cell adhesion and thereby influencing cell migration in an *in vitro* cell culture model. Expression and localization of β -catenin in normal and cancerous human salivary gland cells were evaluated using immunofluorescence and immunoblotting techniques, both with and without the influence of a Wnt

inhibitor (IWR-1). Two and three-dimensional migration assays were also performed. As expected, our data indicate that β -catenin is preferentially localized in the nucleus of cancer cells as compared with normal salivary gland cells, and this expression is significantly decreased under the influence of IWR-1. Both 2D and 3D migration assays revealed that Wnt inhibition limits the migration of cancer cells. We confirm that salivary gland cancer cells exhibit significantly increased β -catenin, which indirectly regulates loss of intercellular adhesion, and potentially enhances cell migration. Inhibition of the Wnt pathway limited migration and could be a potent target to abrogate salivary gland cancer progression.

Key Words: β -catenin; Wnt; Salivary gland cancer; Migration; Progression

INTRODUCTION

Salivary gland carcinomas (SGCs) account for approximately 6% of all head and neck cancers in the United States. They include more than 30 types of benign or malignant neoplasms with variable morphological and physiological traits (1). These traits can be extremely diverse between tumor types and even within individual tumors, thus making SGCs difficult to diagnose and manage. Standard treatment for localized SGCs is surgical excision with or without radiation therapy (1-3). If regional or distant metastases have occurred, therapeutic intervention becomes more limited and survival rates diminish to approximately 40% (4). Additionally, even with judicious intervention, the rate of recurrence for patients with SGCs is high (1). Therefore, identifying markers for early diagnosis and recognizing molecular mechanisms associated with tumor advancement are critical for improving SGC management.

The Wnt signaling pathways have been associated with epithelial-mesenchymal transition (EMT), cellular proliferation and differentiation, and with stem cell populations in multiple types of cancers (5,6). In the canonical pathway, Wnt signaling is dependent on β -catenin, a modulator of gene expression, through nuclear localization and removal of transcriptional repression from Groucho/T-cell factor (TCF)/Lymphoid enhancing factor (LEF) (7). Under normal circumstances, β -catenin is rapidly degraded through a destruction complex when not associated with cadherin-mediated adhesion (8). β -catenin uses the same binding interface to engage both cadherins and TCF, with greater affinity toward the cadherin-catenin interaction. Thus, E-cadherin expression sets a baseline threshold for Wnt/ β -catenin signaling through normal sequestration of β -catenin (9). However, loss of E-cadherin expression, increased Wnt signaling, or mutations associated with components of the destruction complex can lead to expression of cancer related genes associated with tumor progression, metastasis, and invasive phenotypes (10,11). β -catenin expression has also been reported in several types of SGCs including benign and malignant phenotypes (12-18), however, findings were not conclusive across all studies. In two reports, predominant cytoplasmic β -catenin localization with reduced membranous expression was associated with decreased survival, invasiveness, aggressive behavior, and/or a lack of differentiation among malignant tumors (12,17). While in another study, aberrant nuclear localization was suggested to be a contributing factor to the aggressive behavior of epithelial-myoepithelial carcinomas (15). However, neither cytoplasmic nor nuclear localization alone denote malignancy, based on expression also occurring in benign salivary gland tumors (12). Based on this inconsistency among studies, there may be a morphological and behavioral effect from Wnt and β -catenin that differs among salivary gland neoplasms.

The aim of the present study was to evaluate expression of β -catenin in an *in vitro* model of salivary epidermoid carcinoma using the HTB-41 cell line. We also aim to investigate the effects of inhibiting the Wnt/ β -catenin signaling pathway on cellular functions that affect cancer progression, including cell proliferation and migration.

MATERIALS AND METHODS

Human cell lines

A normal salivary gland cell line, HSG, was received as a generous gift (Dr. M. Hoffman, NIH, Bethesda, MA). A submaxillary salivary gland cancer cell line, HTB-41, was acquired from the American Type Culture Collection (ATCC, Manassas, VA). HSG and HTB-41 cells were aseptically cultured in DMEM/F-12 and McCoys5A media respectively (Corning Cellgro, Manassas, VA), supplemented with 10% FBS and 1% penicillin-streptomycin-amphotericin, in 5% CO₂ atmosphere at 37°C. Cancer HTB-41 cell line was also treated with 10 μ M and 50 μ M of a Wnt inhibitor, IWR-1 (Sigma-Aldrich, St. Louis, MO) for 48 hours, and designated as HTB-41/IWR. All cell culture experiments were carried out in triplicate.

Immunofluorescence

HSG, HTB-41, and HTB-41/IWR cells were aseptically grown on tissue culture grade glass coverslips in sterile 12-well plates. On reaching 80% confluence, cells were fixed in 3% paraformaldehyde, and processed for immunofluorescence and confocal imaging. Fixed cells were permeabilized in 0.2% Triton X-100 and blocked with 10% blocking solution for 1 hour. Cells were incubated overnight at 4°C, in anti β -catenin, anti Axin, and anti p-GSK3 β primary antibodies (1:100; Santa Cruz Biotechnology, Inc., Dallas, TX). Following thorough washes with 0.07M PBS, donkey anti-mouse secondary antibody (Dylight 488; 1:200, Jackson ImmunoResearch Laboratories Inc., West Grove, PA) was used to tag the specific proteins of interest. Cells were incubated with Rhodamine-Phalloidin to visualize the actin cytoskeleton (1:50; Cytoskeleton Inc., Denver, CO). Coverslips were mounted with mounting medium containing DAPI for nuclear counterstain (ProLong Gold, Life Technologies, Grand Island, NY). Immunofluorescence images were acquired using a Confocal microscope (Olympus Fluoview FV300, Leeds Precision Instruments, MN).

Western blotting

HSG, HTB-41, and HTB-41/IWR cells were aseptically cultured in 100 mm sterile culture dishes till they reached 90% confluence. Total proteins were extracted using M-PER mammalian protein extraction reagent (Thermo Scientific/Pierce, Rockford, IL). Total proteins were also extracted from

Department of Growth, Development and Structure, SIU School of Dental Medicine, 2800 College Ave, Bldg. 286, Alton, IL 62002, USA

Correspondence: Dr Anita Joy, Department of Growth, Development and Structure, SIU School of Dental Medicine, 2800 College Ave, Bldg. 286, Alton, IL 62002, USA, Telephone 6184747028, e-mail: ajoy@siue.edu

Received: October 10, 2018, Accepted: November 28, 2018, Published: December 03, 2018



This open-access article is distributed under the terms of the Creative Commons Attribution Non-Commercial License (CC BY-NC) (<http://creativecommons.org/licenses/by-nc/4.0/>), which permits reuse, distribution and reproduction of the article, provided that the original work is properly cited and the reuse is restricted to noncommercial purposes. For commercial reuse, contact reprints@pulsus.com

HSG* cells (HSG*=normal HSG cells cultured in cancer secretome). Protein estimation was carried out using the RC DC protein assay (Bio-Rad, Hercules, CA) and equal amounts of protein were resolved by 10% SDS-PAGE under reducing conditions. After electrophoresis, proteins were electrotransferred onto nitrocellulose membranes (Bio-Rad, Hercules, CA), blocked with 5% non-fat milk in 1X PBS, and probed with anti β -catenin, anti E-cadherin, anti Axin, and anti p-GSK3 β antibodies (1:500; Santa Cruz Biotechnology, Dallas, TX). HRP-conjugated goat anti-mouse IgG was used as secondary antibody (1:10,000; Sigma-Aldrich, St. Louis, MO) and Clarity western ECL (Bio-Rad, Hercules, CA) was used as the substrate for HRP detection.

To determine equal protein loading, each membrane was carefully washed, treated for 5 minutes with stripping buffer (Thermo Scientific/Pierce, Rockford, IL) to eliminate the previous reaction and washed with PBS. Membranes containing whole protein were processed as above with anti-tubulin primary antibody (1:10,000; Sigma-Aldrich, St. Louis, MO) and HRP-conjugated goat anti-mouse IgG secondary antibody (1:10,000; Sigma-Aldrich, St. Louis, MO). Chemiluminescent detection was carried out for HRP detection, as described above.

2-Dimensional cell migration assay

HSG, HTB-41, and HTB-41/IWR cells were seeded on sterile, culture-grade glass coverslips, and grown to confluence. A uniform “scratch” was created in a straight line using a sterile micropipette tip on Day 0. Cells were gently washed with 1X PBS to remove any debris, respective growth media was replaced in each well, and incubated at 37°C in a 5% CO₂ environment. Starting at Day 0, images of the “scratch” were acquired from the same field every 24 hours, using an inverted microscope (Nikon Eclipse E600; Nikon, Melville, NY), until the “scratch” was completely eliminated by migrating cells. The experiment was repeated in triplicate.

3-Dimensional cell migration assay

HSG, HTB-41, and HTB-41/IWR cells were incubated in 1 μ M of CM-Dil (Life Technologies, Grand Island, NY) tracking dye as per manufacturer’s instructions. Cells were washed in 1X PBS and resuspended in respective serum-free media. Sterile, culture-grade glass cover slips were placed at the bottom of each well of 6-well transwell plates. 500 μ l of DMEM/F-12 serum-free media was added in the basolateral chamber and HSG cell suspension in 2 ml DMEM/F-12 serum-free media was added to the central well. Transwell plates were incubated at 37°C in a 5% CO₂ environment for 4- and 24-hour time points, and cover slips were imaged using confocal microscopy and cell counts performed (Olympus FluoView FV300, Leeds Precision Instruments, MN) to quantify the adherent labeled cells. The experiment was repeated in triplicate and statistical analyses were performed.

RESULTS

Preferential nuclear localization of β -catenin in salivary gland cancer was abrogated following treatment with Wnt inhibitor. Immunofluorescence studies against β -catenin was carried out using normal human salivary gland cells (HSG) and human cancer salivary gland cells (HTB-41) and is depicted in Figure 1.

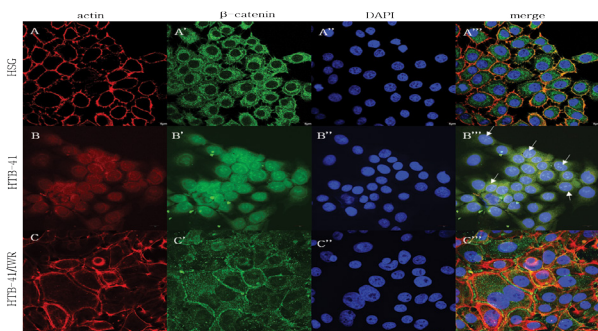


Figure 1) β -catenin translocates into the nucleus in human salivary gland cancer cells. Representative confocal images of HSG, HTB-41, and HTB-41/IWR cells depict localization of β -catenin. (Scale bar=5 μ M)

A, A', A'', merge: Representative confocal images depict actin cytoskeleton, intracellular localization of β -catenin, and nuclei in normal HSG cells. The actin cytoskeleton and cortical actin clearly shows the normal, expected cell morphology of human salivary gland cells. β -catenin is localized to the cell membrane as well as the cytoplasm. The merged image shows β -catenin co-localizing with actin, in the cell membrane but not in the cytoskeleton.

B, B', B'', merge: Representative confocal images depict actin cytoskeleton, intracellular localization of β -catenin, and nuclei in cancer HTB-41 cells. The cytoplasm of cancer cells is filled with β -catenin and translocation into the nucleus is pronounced.

C, C', C'', merge: Representative confocal images depict actin cytoskeleton, intracellular localization of β -catenin, and nuclei in cancer HTB-41 cells following treatment with a Wnt inhibitor. Wnt inhibition abrogates the excessive intracellular accumulation of β -catenin and its nuclear translocation that is seen in cancer cells with an activated Wnt pathway. β -catenin is seen present in the cytoplasm, as well as outlining cell boundaries.

As expected, β -catenin is seen present in the cytoplasm and outlining the borders of normal cells, where it co-localizes with actin (Figures. 1A' and 1A'''). In cancer cells, β -catenin is strongly expressed within the cytoplasm, with no significant localization on the cell membranes. In addition, robust translocation into the nucleus is also clearly seen in cancer cells (Figures 1B' and 1B'''). Following treatment of salivary gland cancer cells with 10 μ M IWR-1, a Wnt inhibitor, β -catenin no longer translocated into the nucleus, rather, a cytoplasmic expression coupled with membrane localization, as expected in normal cells can be seen (Figure 1C' and 1C''').

Western blot analyses to evaluate overall levels of β -catenin showed significantly higher levels of the protein in cancer salivary gland cells as compared to normal cells, which were then significantly decreased following treatment with the Wnt inhibitor (Figure 2).

Cancer cells exhibited altered expression of β -catenin destruction complex components.

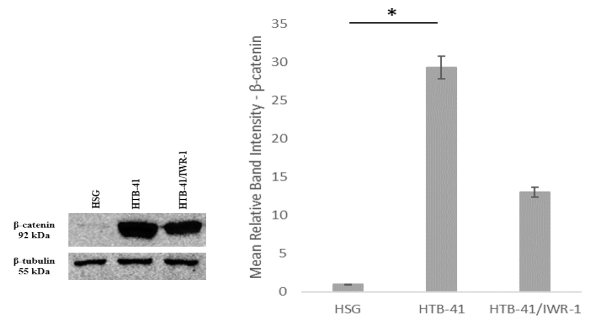


Figure 2) Evaluation of β -catenin expression in HSG, HTB-41, and HTB-41/IWR cells in Western Blot detection at 72 hours. Western blot revealed that β -catenin levels were elevated in cancer cells compared to normal cells, and following Wnt inhibition returned to lower levels. Analyses of relative band intensities followed by a student’s t-test revealed that β -catenin was significantly elevated in cancer cells. Although levels decreased compared to cancer cells following treatment with the Wnt inhibitor, they were not significant. (* p \leq 0.03; data expressed as mean \pm SD)

Axin and phosphorylated glycogen synthase kinase-3 β (p-GSK3 β) form part of the β -catenin destruction complex and are found located in the cytoplasm in normal salivary gland cells (Figures 3A', 3A''', 4A', and 4A'''). In cancer cells, with the activation of the Wnt pathway, the β -catenin destruction complex is dismantled, resulting in decreased expression of Axin and p-GSK3 β in the cytoplasm (Figures 3B', 3B''', Figures 4B', and 4B'''). Inhibition of Wnt using 10 μ M IWR-1 results in normal expression of p-GSK3 β and a minimal change in distribution of Axin in the cancer cells (Figures 3C', 3C''', 4C', and 4C''').

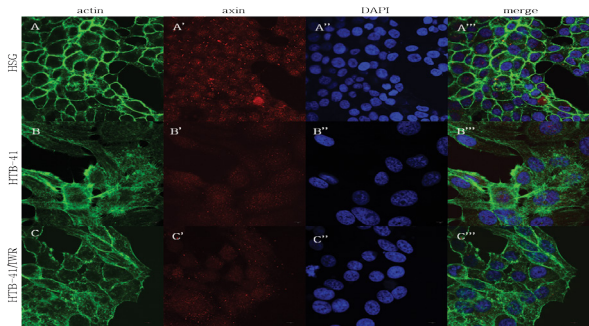


Figure 3) Axin, part of the β -catenin destruction complex, moves out of the cytoplasm in cancer cells. Representative confocal images of HSG, HTB-41, and HTB-41/IWR cells depict localization of Axin. (Scale bar=5 μ M)

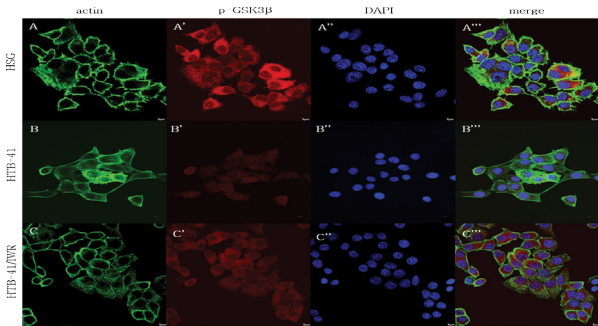


Figure 4) Expression of phosphorylated GSK3β (p-GSK3β), part of the β-catenin destruction complex, is decreased in cancer cells. Representative confocal images of HSG, HTB-41, and HTB-41/IWR cells depict localization of p-GSK3β. (Scale bar=5 μM)

A, A', A", merge: Representative confocal images depict actin cytoskeleton, intracellular localization of Axin, and nuclei in normal HSG cells. Axin shows a punctate presentation within the cytoplasm of normal salivary gland cells.

B, B', B", merge: In cancer cells, although Axin continues to be seen in the cytoplasm, it is no longer present as discrete punctae, but rather is seen as being dispersed.

C, C', C", merge: Following treatment with the Wnt inhibitor, Axin seems to resume its punctate intracellular expression.

A, A', A", merge: Representative confocal images depict actin cytoskeleton, intracellular localization of Axin, and nuclei in normal HSG cells. p-GSK3β shows a strong presentation within the cytoplasm of normal salivary gland cells, where it is present as part of the β-catenin destruction complex.

B, B', B", merge: In cancer cells, there seems to be a significant decrease in p-GSK3β in the cytoplasm.

C, C', C", merge: Following treatment with the Wnt inhibitor, p-GSK3β seems to exhibit resurgence within the cytoplasm.

Western blot analyses to quantify levels of Axin and p-GSK3β revealed decreased levels in cancer states as compared to normal salivary gland cells, followed by a significant reversal to normal levels of p-GSK3β and no reversal in Axin levels following inhibition of the Wnt pathway (Figure 5).

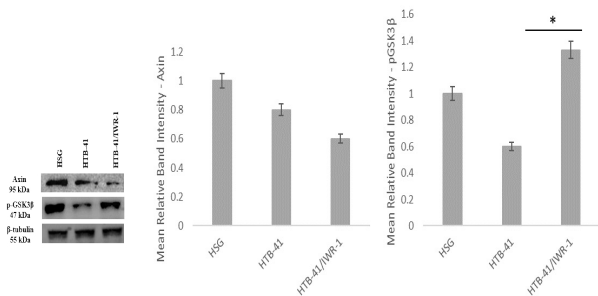


Figure 5) Evaluation of Axin and p-GSK3β expression in HSG, HTB-41, and HTB-41/IWR cells in Western Blot detection at 72 hours. Data revealed that Axin and p-GSK3β levels decreased in cancer cells compared to normal cells. Following Wnt inhibition p-GSK3β returned to almost normal levels while Axin continued to decrease. Analyses of relative band intensities followed by a student's t-test revealed that following treatment with the Wnt inhibitor p-GSK3β levels significantly increased as compared to that in cancer cells. (*p ≤ 0.02; data expressed as mean ± SD).

Wnt inhibition limited migration in human salivary gland cells

A 2-dimensional gap/wound closure assay was carried out to evaluate migration of salivary gland cancer cells. Normal cells migrated to close the gap/wound (approximately 0.5 mm) within four days, while cancer cells migrated at a faster rate to eliminate a gap/wound that was four times wider (approximately 2.0 mm) within two days (Day 4 image not shown due to complete wound closure at Day 3). Essentially, cancer cells migrated eight times faster than normal SG cells. Following inhibition of Wnt by 10 μM

IWR-1, cancer salivary gland cells showed reduced migration rates, with the gap/wound not completely closing even after the fourth day (Figure 6).

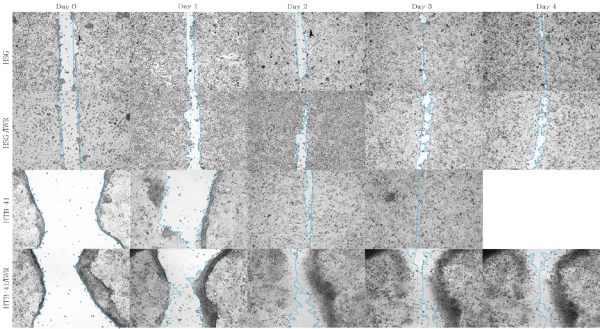


Figure 6) The increased migration exhibited by human salivary gland cancer cells is reversed under the influence of Wnt inhibition. HSG, HTB-41, and HTB-41/IWR cells were cultured till they reached 90% confluency. A uniform "scratch" was created with a sterile micropipette tip on Day 0 (blue dotted lines depict the "gap" or "cell-free" region). Cells were imaged every 24 hours post-Day 0 (4x magnification). HSG cells migrated and almost infiltrated the "scratch" by Day 4. HTB-41 cells migrated at a faster rate than HSG cells to obliterate the "scratch" by Day 3 (Day 4 image is not shown due to the complete closure by Day 3). Following Wnt inhibition, cancer HTB-41 cells did not eliminate the gap even after four days. Normal cells when treated with the Wnt inhibitor also showed decreased migration

A 3-dimensional migration assay showed that cancer salivary gland cells migrated at a significantly faster rate as compared to normal salivary gland cells. Following treatment with the Wnt inhibitor, cancer cell migration rates were significantly decreased (Figure 7).

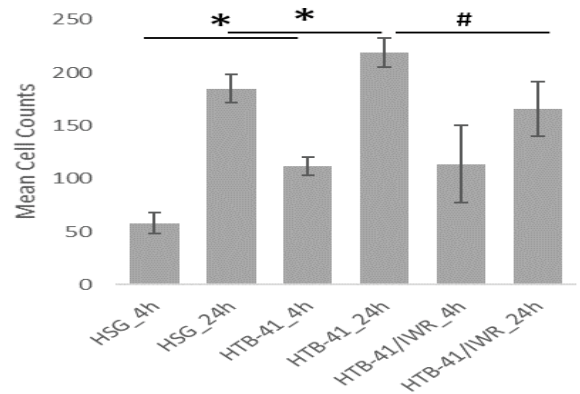


Figure 7) Data from 3-D Migration Transwell Assays at 4 and 24 hours reveal that Wnt inhibition abrogates the enhanced migration seen in human salivary gland cancer cells. As expected, cancer cells exhibited significantly faster migration compared to normal cells as early as 4 hours (p ≤ 0.0001) and continued to do so at 24 hours (p ≤ 0.0001). Following treatment with the Wnt inhibitor, cancer cells showed significant decrease in migration by 24 hours (p ≤ 0.0003). (*p ≤ 0.0001, #p ≤ 0.0003; data expressed as mean ± SD).

DISCUSSION

Ample evidence supports the idea that Wnt/β-catenin signaling is associated with resistance to chemotherapy, acquisition of epithelial-mesenchymal transition (EMT) features and is being studied as a potential therapeutic target in various cancers (5). Within a cell, β-catenin is known to play a dual role - as a linker protein in cell-cell adhesion, and as a component of the Wnt signaling pathway. In association with the catenins, E-cadherin exhibits its normal cellular adhesive function and sequestration of β-catenin (19). When the canonical Wnt pathway is activated, β-catenin, which normally undergoes phosphorylation/ubiquitination via targeting by a destruction complex (adenomatous polyposis coli (APC) + casein kinase-β (CK1β) + pGSK3β + Axin [main] and yes-associated protein/transcriptional co-activator with PDZ-binding motif (YAP/TAZ) + β-transducin repeat-containing protein (β-TrCP) [secondary]) is not proteasomally degraded. Instead, β-catenin begins to accumulate in the cytoplasm with eventual translocation into the nucleus, and subsequent displacement of the transducing-like enhancer of split (TLE)/Groucho repression complex from TCF/LEF (6). Thus, in its dual role, β-catenin can function through the Wnt signaling pathway or through the E-cadherin catenin complex.

Wnt related mutations have been shown to influence the initial development and the progression of several types of cancers, including carcinomas of the gastrointestinal tract, lungs, ovaries, uterus, thyroid, and pancreas (20-22). There is also mounting evidence that this pathway also contributes to tumorigenesis in salivary gland cancers, and inhibition of Wnt has been postulated as a potential mechanism to limit cancer progression. Here increased β -catenin activation, in combination with cAMP response element (CREB)-binding and mixed-lineage leukemia (MLL) proteins, has been associated with promoter methylation of self-renewal genes in salivary gland cancer (13). Furthermore, regulatory changes of Wnt, β -catenin, and Wnt inhibitory factor-1 have been linked to the development and/or progression of pleomorphic adenomas, and more invasive adenoid cystic carcinoma (14,19-24). Similarly, mutations of CTNNB1 (β -catenin), Axin1, Axin2, and APC have been shown in adenoid cystic carcinoma and basal cell adenoma (25,26). While our results are consistent with data showing immunofluorescence localization of β -catenin at cell-cell interfaces and within the cytoplasm of epidermoid carcinoma to Sengupta et al., we also observed nuclear translocation (27). This observation is supported by Chen et al., where Western Blot analysis of nuclear fractions revealed the presence of β -catenin and is consistent with immunohistochemical data from other studies (28,29). In addition, nuclear β -catenin could be abrogated when cells were treated with the Wnt inhibitor IWR-1. Concurrently, total protein concentration was also shown to decrease following treatment. These results are similar to previous studies using L-Wnt3a cells, osteosarcoma cell lines, colorectal and pancreatic cancer cells, and mouse epiblast stem cells where introduction of IWR inhibitors alone or in combination with a GSK3 inhibitor (CHIR) knocked down protein expression of β -catenin and caused cytoplasmic retention respectively (30-34). Furthermore, we observed no significant change in abatement between use of 10 μ M and 50 μ M doses of IWR-1. It is expected that upon further analysis of protein lysates between control, cancer, and treated groups we would observe a reduction in nuclear localization of β -catenin with an expected increase in phosphorylated β -catenin when IWR-1 is present.

In the case of the components of the β -catenin destruction complex, namely Axin1 and p-GSK3 β , their distributions were not overtly altered following Wnt inhibition. Levels of Axin1 were not significantly altered between treated and untreated HTB-41 groups, while levels of p-GSK3 β were prominently increased following Wnt inhibition between these same groups. Our data indicate higher levels of Axin1 in normal salivary gland cells than in the cancer cells, both in the cytoplasm and as clear specks on the cell membrane. Although our immunofluorescence data show a more distinct localization of Axin1 in the cytoplasm of cancer cells and increased representation on the cell membrane following Wnt inhibition, levels did not significantly change in cancer cells when compared to control or treated groups. We speculate that this might be associated with the mechanism of action associated with IWR-1. As shown by Bao et al., Axin1 is stabilized in MDA-MB-231 breast cancer cells following treatment with 10 μ M of inhibitor (35). Here, Wnt signaling was inhibited with no alteration to tankyrase1/2, molecules that bind to a conserved domain on Axin1 and promote degradation. Further support is shown in a study conducted by Mashima et al., where Axin1 protein expression in colorectal cancer cells was unchanged when subjected to 3 and 9 μ M of IWR-1 (31). This study further suggests that the salivary cancer cell line in use in our study may not be tankyrase inhibitor resistant, as we did not see similar trends to their COLO-320IWR cell line, where there was a coordinated increase in expression of both Axin1 and Axin 2. We would expect that on probing of protein lysates, Axin2 would also be increased in our cancer cell line when treated with IWR-1, though further testing is needed to verify. Finally, it is also likely that the change in protein expression levels between HSG and HTB-41 cells are due to variable expression between cell types, and no significance between cancer and cancer treated cells being associated with the reported rate-limiting role of Axin1 on the destruction complex (36-38).

Expression levels of p-GSK3 β significantly increased following treatment with IWR-1, with a mean intensity higher than that of the normal salivary gland cells used. This was an unexpected result as Cross, et al. reported GSK3 β phosphorylation at Ser-9 caused inactivation, and Fei, et al. showed subsequent β -catenin stabilization, nuclear accumulation, and enhanced Wnt signaling (39,40). IWR-1 has also been shown to significantly decrease levels or inhibit activity of p-GSK3 β in non-small cell lung cancer and microvascular endothelial cells (41,42). However, other studies using retinal epithelial cells and skin fibroblasts found little expression difference between IWR-1 treated and control groups (43,44). These discrepancies between studies would suggest the role of IWR-1 on modulation of p-GSK3 β might be cell type specific as shown in the previous information, or other signaling

pathways might be influencing phosphorylation of GSK3 β . In Mishra, et al. expression levels of GSK3 β and β varied among different types of oral cancers, with p-GSK3 β also varying among tissue samples (45). Alternatively, phosphorylation of GSK3 β and β may also occur independently of Wnt signaling through insulin, platelet derived growth factor, fibroblast growth factor, epidermal growth factor, or reelin (46-49). However, it is worth noting that GSK-3 activity in the destruction complex has been shown to be impervious to Ser-9 phosphorylated inactivation when bound to Axin (50). Therefore, it seems that only unbound GSK-3 β is phosphorylated, leaving the very small cellular fraction that does associate with the Axin destruction complex active.

Finally, in addition to its effect on the destruction complex components and β -catenin in particular, IWR-1 use resulted in a significant decrease in cancer cell migration. Our data indicates both 2-dimensional cell migration rates and 3-dimensional cell invasion rates were significantly decreased in cancer cells following inhibition. These findings are not atypical, as other studies using IWR-1 have shown similar outcomes on cell migration, proliferation, and invasiveness in multiple cell types (35,44,51,52).

CONCLUSION

In summary, we have shown that inhibition of the Wnt pathway through use of IWR-1, can suppress nuclear localization of β -catenin, and cellular migration and invasiveness of HTB-41. This work helps to establish a link between the Wnt pathway and progression of epidermoid salivary gland carcinoma *in vitro*. Furthermore, it helps to establish the potential usage of Wnt inhibitors in treatment of oral cancers. However, further studies are required to determine the full involvement of the Wnt pathway in progression of HTB-41 and other oral cancers.

CONFLICTS OF INTEREST

The authors do not declare any conflict of interest for this work.

ACKNOWLEDGEMENTS

This study was supported by the SIU SDM Dean's Summer Student Research Fellowships awarded to J. Welborn and A. Altman (DSSR15-02 and DSSR15-03/Joy: PI), and a SIU SDM Pilot Project Award to A. Joy (PP16-02).

REFERENCES

1. Barnes L, Eveson JW, Reichart P, et al. World Health Organization Classification of Tumours: Pathology and genetics of head and neck tumours. IARC Press: Lyon 2005.
2. Stenman G, Persson F, Andersson MK. Diagnostic and therapeutic implications of new molecular biomarkers in salivary gland cancers. *Oral Oncol.* 2014;50:683-90.
3. Namboodiripad PC. A review: Immunological markers for malignant salivary gland tumors. *Journal of Oral Biol Craniofacial Res.* 2014;4:127-34.
4. Guzzo M, Locati LD, Prott FJ, et al. Major and minor salivary gland tumors. *Crit Rev Hematol.* 2014;74:134-48.
5. Duchartre Y, Kim Y, Kahn M. The Wnt signaling pathway in cancer. *Crit Rev Hematol.* 2016;66:141-49.
6. Zhan T, Rindtorff N, Boutros M. Wnt signaling in cancer. *Oncogene.* 2017;36:1461-73.
7. Miller RK, Hong JY, Munoz WA, et al. Beta-catenin versus the other catenins: assessing our current view of canonical Wnt signaling. *Progress in Molecular Biol Translat Sci.* 2013;116:387-407.
8. McCrea PD, Maher MT, Gottardi CJ. Nuclear signaling from cadherin adhesion complexes. *Current Topics Develop Biol.* 2015;112:129-96.
9. Jeanes A, Gottardi CJ, Yap AS. Cadherins and cancer: how does cadherin dysfunction promote tumor progression? *Oncogene.* 2008;27:6920-29.
10. Hajra KM, Fearon ER. Cadherin and catenin alterations in human cancer. *Genes Chromosomes Cancer.* 2002;34:255-68.
11. Moon RT, Kohn AD, De Ferrari GV. Wnt and α -catenin signaling: diseases and therapies. *Nature Rev Genet.* 2004;5:691-701.

12. Chandrashekar C, Angadi PV, Krishnapillai R. α -catenin expression in benign and malignant salivary gland tumors. *Int J Surg Pathol*. 2011;19:433-40.
13. Wend P, Fang L, Zhu Q, et al. Wnt/ α -catenin signaling induces MLL to create epigenetic changes in salivary gland tumours. *The EMBO J*. 2013;32:1977-89.
14. Wang R, Geng N, Zhou Y, et al. Aberrant Wnt-1/ β -catenin signaling and WIF-1 deficiency are important events which promote tumor cell invasion and metastasis in salivary gland adenoid cystic carcinoma. *Bio-Med Mat Eng*. 2015;26:2145-53.
15. Furuse C, Cury PR, Altemani A, et al. α -catenin and E-cadherin expression in salivary gland tumors. *Int J Surg Pathol* 2006;14:212-17.
16. Wilson TC, Ma D, Tilak A, et al. Next-generation sequencing in salivary gland basal cell adenocarcinoma and basal cell adenoma. *Head Neck Pathol*. 2016;10:494-500.
17. Lill C, Schneider S, Seemann R, et al. Correlation of α -catenin, but not PIN1 and cyclin D1, overexpression with disease-free and overall survival in patients with cancer of the parotid gland. *Head and Neck*. 2015;37:30-6.
18. Tesdahl BA, Wilson TC, Hoffman HT, et al. Epithelial-mesenchymal transition protein expression in basal cell adenomas and basal cell adenocarcinomas. *Head Neck Pathol*. 2016;10:176-81.
19. Chen GT, Waterman ML. Cancer: leaping the E-cadherin hurdle. *The EMBO J*. 2015;34:2308-9.
20. Giles RH, van Es JH, Clevers H. Caught up in a Wnt storm: Wnt signaling in cancer. *Biochim Biophys Acta*. 2003;1653:1-24.
21. Collu GM, Hidalgo-Sastre A, Brennan K. Wnt-Notch signaling crosstalk in development and disease. *Cellul Molec Life Sci*. 2014;71:3553-67.
22. van Es JH, Clevers H. Notch and Wnt inhibitors as potential new drugs for intestinal neoplastic disease. *Trends Molec Med* 2005;11:496-502.
23. Queimado L, Lopes CS, Reis AM. An inhibitor of the Wnt pathway is rearranged in salivary gland tumors. *Genes Chromosomes Cancer*. 2007;46:215-55.
24. Ramachandra I, Ganapathy V, Gillies E, et al. Wnt inhibitory factor 1 suppresses cancer stemness and induces cellular senescence. *Cell Death and Disease*. 2014;5:1246.
25. Sato M, Yamamoto H, Hatanaka Y, et al. Wnt/ β -catenin signal alteration and its diagnostic utility in basal cell adenoma and histologically similar tumors of the salivary gland. *Pathology – Research and Practice*. 2018.
26. Daa T, Kashima K, Kaku N, et al. Mutations in components of the Wnt signaling pathway in adenoid cystic carcinoma. *Modern Pathol*. 2004;17:1475-82.
27. Sengupta PK, Bouchie MP, Kukuruzinska MA. N-Glycosylation gene DPAGT1 is a target of the Wnt/ β -catenin signaling pathway. *The J Biol Chem*. 2010;285:31164-73.
28. Chen L, Liu D, Chang J, et al. Methylation status of insulin-like growth factor binding protein 7 concurs with the malignance of oral tongue cancer. *J Exp Clin Cancer Res* 2015;34:20.
29. Prakash S, Swaminathan U, Nagamalani BR, et al. Beta-catenin in disease. *J Oral Maxillofacial Pathol*. 2016;20:286-99.
30. Chen B, Dodge ME, Tang W, et al. Small molecule mediated disruption of Wnt-dependent signaling in tissue regeneration and cancer. *Nature Chem Biol*. 2009;5:100-07.
31. Martins-Neves SR, Paiva-Oliveira DI, Fontes-Riberiro C, et al. IWR-1, a tankyrase inhibitor, attenuates Wnt/ β -catenin signaling in cancer stem-like cells and inhibits in vivo the growth of a subcutaneous human osteosarcoma xenograft. *Cancer Letters*. 2018;414:1-15.
32. Kim H, Wu J, Ye S, et al. Modulation of α -catenin function maintains mouse epiblast stem cell and human embryonic stem cell self-renewal. *Nature Communications*. 2013;4:2403.
33. Sarkar S, Mandal C, Sangwan R, et al. Coupling G2/M arrest to the Wnt/ α -catenin pathway restrains pancreatic adenocarcinoma. *Endocrine-Related Cancer*. 2014;21:113-25.
34. Mashima T, Taneda Y, Jang M, et al. mTor signaling mediates resistance to tankyrase inhibitors in Wnt-driven colorectal cancer. *Oncotarget*. 2017;8:47902-15.
35. Bao R, Christova T, Song S, et al. Inhibition of tankyrases induces Axin stabilization and blocks Wnt signaling in breast cancer cells. *PLOS One*. 2012;7:11.
36. Tan CW, Gardiner BS, Hirokawa Y, et al. Wnt signaling pathway parameters for mammalian cells. *PLOS One*. 2012;7:2.
37. MacDonald BT, Tamai K, He X. Wnt/ β -catenin signaling: components, mechanisms, and diseases. *Develop Cell*. 2009;17:9-26.
38. Kitazawa M, Hatta T, Ogawa K, et al. Determination of rate-limiting factor for formation of β -catenin destruction complexes using absolute protein quantification. *J Proteome Res*. 2017;16:3576-84.
39. Fei Y, Xiao L, Doetschman T, et al. Fibroblast growth factor 2 stimulation of osteoblast differentiation and bone formation is mediated by modulation of the Wnt signaling pathway. *J Biol Chem*. 2011;286:40575-83.
40. Cross DA, Alessi DR, Cohen P, et al. Inhibition of glycogen synthase kinase-3 by insulin mediated by protein kinase B. *Nature*. 1995;378:785-9.
41. Liu Y, Yang S, Li M, et al. Tumorigenesis of smoking carcinogen 4-(methylnitrosamino)-1-(3-pyridyl)-1-butanone is related to its ability to stimulate thromboxane synthase and enhance stemness of non-small cell lung cancer stem cells. *Cancer Lett*. 2016;370:198-206.
42. Xu Y, Zhang J, Jiang W, et al. Astaxanthin induces angiogenesis through Wnt/ β -catenin signaling pathway. *Phytomedicine*. 2015;22:744-51.
43. Wang Y, Sang A, Zhu M, et al. Tissue factor induces VEGF expression via activation of the Wnt/ β -catenin signaling pathway in ARPE-19 cells. *Molecule Vision*. 2016;22:886-97.
44. Wang X, Zhu Y, Sun C, et al. Feedback activation of basic fibroblast growth factor signaling via the Wnt/ β -catenin pathway in skin fibroblasts. *Front Pharmacol*. 2017;8:32.
45. Mishra R, Nagini S, Rana A. Expression and inactivation of glycogen synthase kinase 3 α / β and their association with the expression of cyclin D1 and p53 in oral squamous cell carcinoma progression. *Mol Cancer*. 2015;14:20.
46. Ding VW, Chen R, McCormic F. Differential regulation of glycogen synthase kinase 3 β by insulin and Wnt signaling. *J Bio Chem*. 2000;275:32475-81.
47. Basu D, Lettan R, Damodaran K, et al. Identification, mechanism of action, and antitumor activity of a small molecule inhibitor of Hippo, TGF- α , and Wnt signaling pathways. *Mol Cancer Therap*. 2014;13:1457-67.
48. Mishra R. Glycogen synthase kinase 3 beta: can it be a target for oral cancer. *Mol Cancer* 2010;9:144.
49. Manoukian AS, Woodgett JR. Role of glycogen synthase kinase-3 in cancer: regulation by Wnt and other signaling pathways. *Adv Cancer Res*. 2002;84:203-29.
50. Beurel E, Grieco SF, Jope RS. Glycogen synthase kinase-3 (GSK3): regulation, actions, and diseases. *Pharmacol Therap*. 2015;1:114-31.
51. Lee SC, Kim O, Lee SK, et al. IWR-1 inhibits epithelial-mesenchymal transition of colorectal cancer cells through suppressing Wnt/ α -catenin signaling as well as surviving expression. *Oncotarget*. 2015;6:27146-59.
52. Morizane R, Fujii S, Monkawa T, et al. miR-363 induces transdifferentiation of human kidney tubular cells to mesenchymal phenotype. *Clin Exp Nephrol*. 2015;20:394-401.